

shows that only the LMO's which constitute the reaction centers suffer appreciable deformation during reaction; other LMO's have great transferability. Chemical reactions can thus be deemed as local properties of reactant molecules. The particular LMO's associated with reaction centers reveal a pattern that the reactions of open-shell molecules proceed through a three-stage mechanism. The successive  $\beta$ - and  $\alpha$ -spin electron transfers which take place between reactant molecules should lead to a new electron-pair bond via a three-center bond. The concomitant spin polarization of the old bond plays an important role in the cleavage of that bond. The whole aspect of the reactions is well in accord with the customarily accepted mechanistic scheme. In conclusion, the UHF-LMO treatments do not only shed light on the mechanism of radical reactions, but provide a sound theoretical foundation for conventional concepts already familiar in chemistry.

## References and Notes

- (1) M. J. Feinberg and K. Ruedenberg, *J. Chem. Phys.*, **54**, 1495 (1971).
- (2) R. F. W. Bader and H. J. T. Preston, *Int. J. Quant. Chem.*, **3**, 327 (1969).
- (3) C. W. Wilson and W. A. Goddard III, *Theor. Chim. Acta*, **26**, 195, 211 (1972).
- (4) J. E. Lennard-Jones and J. A. Pople, *Proc. R. Soc. London, Ser. A*, **210**, 190 (1951).
- (5) C. Edmiston and K. Ruedenberg, *Rev. Mod. Phys.*, **35**, 457 (1963); *J. Chem. Phys.*, **43**, 597 (1965).
- (6) K. F. Purcell and T. G. M. Doph, *J. Am. Chem. Soc.*, **94**, 2693 (1972).
- (7) A. Dedieu and A. Veillard, *J. Am. Chem. Soc.*, **94**, 6730 (1972).
- (8) D. A. Dixon and W. N. Lipscomb, *J. Am. Chem. Soc.*, **95**, 2853 (1973).
- (9) D. M. Hirst and M. E. Linington, *Theor. Chim. Acta*, **16**, 55 (1970).
- (10) S. L. Guberman and W. A. Goddard III, *J. Chem. Phys.*, **53**, 1803 (1970).
- (11) K. F. Purcell and W. C. Danen, *J. Am. Chem. Soc.*, **94**, 7613 (1972).
- (12) C. Trindle, *J. Am. Chem. Soc.*, **92**, 3251, 3255 (1970).
- (13) J. A. Pople and R. K. Nesbet, *J. Chem. Phys.*, **22**, 571 (1954).
- (14) J. A. Pople, D. L. Beveridge, and P. A. Dobosh, *J. Chem. Phys.*, **47**, 2026 (1967).
- (15) The expansion coefficients obtained by the present UHF method will be somewhat different from those obtained by the variational configuration interaction method or by the spin-extended Hartree-Fock method, which minimizes the total energy after spin-projection. However, the differences are not so large as to affect seriously the conclusion of this work.
- (16) H. Baba, S. Suzuki, and T. Takemura, *J. Chem. Phys.*, **50**, 7078 (1969).
- (17) K. Morokuma and R. E. Davis, *J. Am. Chem. Soc.*, **94**, 1060 (1972).
- (18) L. C. Snyder and A. T. Amos, *J. Chem. Phys.*, **42**, 3670 (1965).
- (19) A. T. Amos and M. Woodward, *J. Chem. Phys.*, **50**, 119 (1969).
- (20) A. T. Amos and B. L. Burrows, *J. Chem. Phys.*, **52**, 3072 (1970).
- (21) H. Fujimoto, S. Yamabe, T. Minato, and K. Fukui, *J. Am. Chem. Soc.*, **94**, 9205 (1972).
- (22) J. R. Hoyland, *Theor. Chim. Acta*, **22**, 229 (1971).
- (23) In the state correlation diagram, the smooth interchange of spin pairings is considered to be related with the noncrossing of diabatic bases  $\Phi_G$  and  $\Phi_{LE}^+$ .
- (24) As can be conjectured from Figure 4, the back charge transfer process will be much more important in the case of nucleophilic reactions, but immaterial in the case of electrophilic reactions.
- (25) In the case of the insertion-like approach, the contribution of the spin polarization was also greatly reduced, and identical  $\alpha$ -spin densities were induced at the two ends of the substrate bond.
- (26) Importance of the steric effects (exchange-repulsion interactions) has been considered by T. Fueno, S. Nagase, K. Tatsumi, and K. Yamaguchi, *Theor. Chim. Acta*, **26**, 43 (1972); S. Nagase and T. Fueno, *ibid.*, **35**, 217 (1974).

## Solid State Polymerization of $S_2N_2$ to $(SN)_x$ <sup>1</sup>

Marshall J. Cohen,<sup>2a,c</sup> A. F. Garito,<sup>2a,c</sup> A. J. Heeger,<sup>2a,c</sup> A. G. MacDiarmid,<sup>\*2b,c</sup>  
C. M. Mikulski,<sup>2b,c</sup> M. S. Saran,<sup>2b,c</sup> and J. Kleppinger<sup>2b,c</sup>

*Contribution from the Departments of Physics and Chemistry and Laboratory for Research on the Structure of Matter, University of Pennsylvania, Philadelphia, Pennsylvania 19174.*

*Received September 18, 1975*

**Abstract:** A model of the solid state polymerization of  $S_2N_2$  to  $(SN)_x$  is presented using x-ray structure results for  $S_2N_2$ ,  $(SN)_x$ , and a crystal of  $S_2N_2$  which has been allowed to partially polymerize.  $(SN)_x$  has the monoclinic space group  $P2_1/c$  with two crystallographically equivalent chains per unit cell and two SN units per chain:  $a = 4.153$  (6),  $b = 4.439$  (5),  $c = 7.637$  (12) Å, with  $\beta = 109.7$  (1)°. The structure of a single chain consists of nearly equal bond lengths with successive values of 1.593 (5) and 1.628 (7) Å; the NSN and SNS bond angles are 106.2 (2)° and 119.9 (4)°, respectively.  $S_2N_2$  forms in the monoclinic space group  $P2_1/c$  with two  $S_2N_2$  molecules per unit cell:  $a = 4.485$  (2),  $b = 3.767$  (1),  $c = 8.452$  (3) Å, with  $\beta = 106.43$  (3)°. The  $S_2N_2$  molecule is cyclic and nearly square planar with SN bond lengths of 1.657 (1) and 1.651 (1) Å and NSN and SNS bond angles of 89.58 (6)° and 90.42 (6)°, respectively.

## I. Introduction

The past 2 years have witnessed a remarkable growth of interest in polymeric sulfur nitride,  $(SN)_x$ . In 1973, Labes and co-workers<sup>3a</sup> reported on experimental studies of the electrical transport properties which suggested that  $(SN)_x$  was metallic. Heat capacity measurements<sup>3b</sup> in the pumped helium temperature range were consistent with metallic behavior. Since  $(SN)_x$  was known to be a polymer, the electronic properties were assumed to be one dimensional. This assumption coincided with the current interest in the properties of one-dimensional systems exemplified by the charge-transfer salts of (TCNQ)<sup>4</sup> and the platinum-chain salts.<sup>5</sup>

Experimental studies on pure material verified the metallic behavior and demonstrated that it is possible to vacuum deposit oriented epitaxial films of  $(SN)_x$  on a wide range of polymer substrates.<sup>6</sup> These films have a high optical anisotropy throughout the near infrared and the low-frequency portion of the visible spectrum suggesting possible applications in

optical devices.  $(SN)_x$  remains metallic to very low temperatures and becomes superconducting near 0.3 K,<sup>7</sup> thus extending the phenomenon of superconductivity into a new region of the periodic table.

Experimental studies<sup>3,7-9</sup> have shown no indication of the instabilities expected for pseudo-one-dimensional systems. Moreover, optical studies on single crystals and epitaxial films<sup>6b</sup> imply that  $(SN)_x$  is not to be regarded as a one-dimensional, but as an anisotropic two- or possibly three-dimensional, metal. These experimental studies thus suggest relatively strong interactions between polymer chains.

In this communication we report detailed structural information on<sup>10</sup>  $(SN)_x$  obtained using x-ray techniques together with the x-ray determined structures of  $S_2N_2$  and of a crystal of  $S_2N_2$  which has been allowed to partially polymerize. Using these data, a model of the solid state polymerization of  $S_2N_2$  to  $(SN)_x$  is proposed and discussed. The polymerization process implies relatively strong interactions between chains in the  $(SN)_x$  crystal structure.

**Table I.** The Unit Cell Parameters and Atomic Positions of  $S_2N_2$ ,  $(SN)_x$ , and Partially Polymerized  $S_2N_2$  (see Text)

|                     | $S_2N_2$    | $(SN)_x$   |                              | Partially polymerized $S_2N_2$ |
|---------------------|-------------|------------|------------------------------|--------------------------------|
|                     |             | Room temp  | $-145\text{ }^\circ\text{C}$ |                                |
| Structure           | Monoclinic  | Monoclinic | Monoclinic                   | Monoclinic                     |
| Space Group         | $P2_1/c$    | $P2_1/c$   | $P2_1/c$                     | $P2_1/c$                       |
| $a$ , Å             | 4.485 (2)   | 4.153 (6)  | 4.137 (5)                    | 4.460 (4)                      |
| $b$ , Å             | 3.767 (1)   | 4.439 (5)  | 4.431 (4)                    | 3.755 (4)                      |
| $c$ , Å             | 8.452 (3)   | 7.637 (12) | 7.520 (10)                   | 8.470 (9)                      |
| $\beta$ , deg       | 106.43 (3)  | 109.7 (1)  | 109.53 (9)                   | 105.58 (8)                     |
| S–N                 | 1.657 (1)   | 1.593 (5)  | 1.596 (5)                    | 1.650 (4)                      |
|                     | 1.651 (1)   | 1.628 (7)  | 1.638 (6)                    | 1.652 (3)                      |
| Angle               | 90.42 (6)   | 119.9 (4)  | 119.0 (4)                    | 90.6 (2)                       |
| S–N–S, deg          |             |            |                              |                                |
| Angle               | 89.58 (6)   | 106.2 (2)  | 106.2 (2)                    | 89.4 (2)                       |
| N–S–N, deg          |             |            |                              |                                |
| Sulfur <sup>a</sup> |             |            |                              |                                |
| $x$                 | 0.20243 (8) | 0.1790 (8) | 0.1813 (7)                   | 0.2007 (2)                     |
| $y$                 | 0.1210 (1)  | 0.7873 (6) | 0.7874 (5)                   | 0.1190 (3)                     |
| $z$                 | 0.10635 (4) | 0.3443 (4) | 0.3449 (4)                   | 0.1062 (1)                     |
| Nitrogen            |             |            |                              |                                |
| $x$                 | –0.1735 (3) | 0.141 (3)  | 0.143 (3)                    | –0.176 (1)                     |
| $y$                 | 0.0475 (4)  | 0.431 (2)  | 0.429 (2)                    | 0.050 (1)                      |
| $z$                 | 0.0778 (2)  | 0.322 (2)  | 0.325 (1)                    | 0.0770 (5)                     |

<sup>a</sup> The complete structural data including the atomic positions of the interstitial defect sites can be found in the supplementary material.

## II. The Crystal Structures of $S_2N_2$ and $(SN)_x$

The  $(SN)_x$  crystals studied were synthesized and grown via the solid state polymerization of single crystals of  $S_2N_2$  as described earlier.<sup>10,11</sup> Single crystals for x-ray studies were chosen by high quality visual appearance and were subsequently checked for possible twinning. The x-ray molecular and crystallographic structures were determined by the Molecular Structure Corp.<sup>12</sup>

Vapor grown  $S_2N_2$  forms colorless monoclinic crystals with space group  $P2_1/c$  and two molecules per unit cell (Table I). A view of the monoclinic  $S_2N_2$  crystal structure (Figure 1) shows  $S_2N_2$  crystallizes in a herring-bone pattern characteristic of closest packing molecular crystals of flat planar molecules. The  $S_2N_2$  structure was determined at  $-130\text{ }^\circ\text{C}$  using 464 independent reflections leading to a refined structure with an  $R$  factor of 0.03. Typical scans through a Bragg reflection showed an  $\omega$  width of  $0.2^\circ$ . The  $S_2N_2$  molecular structure is cyclic and nearly square planar with SN bond lengths of 1.657 (1) and 1.651 (1) Å and NSN and SNS bond angles of  $89.58(6)^\circ$  and  $90.42(6)^\circ$ , respectively. The nearest sulfur–sulfur and nitrogen–nitrogen intermolecular distances of 3.583 (5) and 3.77 (1) Å, respectively, are comparable to or larger than van der Waals separation distances. However, along the crystallographic  $a$  axis, there is a relatively short intermolecular sulfur–nitrogen contact of 2.890 (1) Å compared with approximately 3.35 Å expected for the corresponding sulfur–nitrogen van der Waals distance. Normal to the  $a$  axis, the shortest intermolecular distance is 3.150 (1) Å, again due to sulfur–nitrogen contact.

$(SN)_x$  forms lustrous golden crystals in the monoclinic system  $P2_1/c$  with two electronically inequivalent chains per unit cell which are identical in structure and whose locations are related by the screw axis symmetry of the space group (Table I). The view of the  $(SN)_x$  structure in Figure 2 shows the polymer chains are oriented along the crystallographic  $b$  axis. This structure was determined both at room temperature and at  $-145\text{ }^\circ\text{C}$  on a crystal which showed only a very few reflections attributable to a twin. The  $(SN)_x$  chains were found to be planar at  $-145\text{ }^\circ\text{C}$  and nearly planar at room temperature, the maximum height of an atom above the average plane

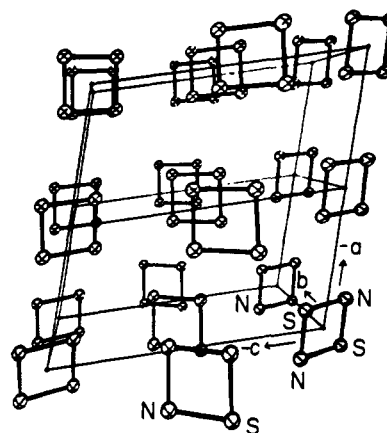


**Figure 1.** The crystal structure of  $S_2N_2$ .

being 0.01 Å. The  $(SN)_x$  chains are parallel to the  $(\bar{1}02)$  plane. Typical scans through a strong reflection show  $\omega$  widths of approximately  $3^\circ$ . This large mosaic spread is probably related to the fibrous nature of the single crystals. The parameters presented in Table I are based on a refinement model which includes the main  $(SN)_x$  chain at 73% occupancy and the sulfur atoms of three minor  $(SN)_x$  chains, arising from the defect structure of the crystal (vide infra), at 9% occupancy each. The nitrogen atoms of these chains could not be located. The inclusion of the three minor disordered sulfur atoms in the final model reduced the unweighted  $R$  factor from 0.165 to 0.111. A single  $(SN)_x$  chain consists of nearly equal S–N bond lengths of 1.593 (5) and 1.628 (7) Å at room temperature, and N–S–N and S–N–S bond angles of  $106.2(2)^\circ$  and  $119.9(4)^\circ$ , respectively. These bond distances and angles are not affected significantly if the disordered sulfur atoms are not considered in the refinement. An additional study of both twins of a twinned crystal of  $(SN)_x$  formed by polymerizing  $S_2N_2$  at room temperature for 6 weeks confirmed these results.

Complete experimental information including data acquisition techniques, the refinement method, and the reflection amplitudes can be found in the supplementary material (see

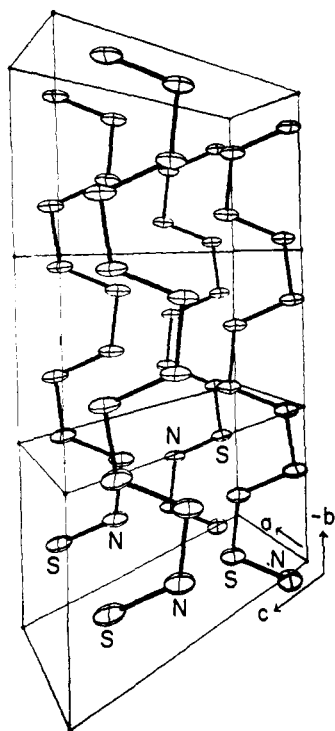


Figure 2. The crystal structure of  $(\text{SN})_x$ .

paragraph at end of paper). These x-ray results differ significantly from the structures obtained previously from electron diffraction studies<sup>13</sup> where difficulties can arise since electron scattering is not well described by the first Born approximation so that multiple scattering effects lead to intensities which are difficult to analyze.

### III. The Polymerization Process

An  $\text{S}_2\text{N}_2$  crystal was stored at 3 °C for 72 h. During this time, the crystal changed to an intense blue-black color and finally became golden in appearance. Fifteen reflections were monitored several times during this period; no changes in the unit cell or x-ray intensity were observed. After an additional week at 3 °C the crystal was warmed to 23 °C for 6 h to promote polymerization. The resultant crystal exhibited the golden luster and striated surface characteristic of  $(\text{SN})_x$ . A full x-ray structure analysis was carried out at -130 °C on this partially polymerized  $\text{S}_2\text{N}_2$ , giving the unit cell parameters listed in Table I. From the decrease in intensities when compared with the same  $\text{S}_2\text{N}_2$  reflections obtained before polymerization, the crystal was found to be only 25% crystalline  $\text{S}_2\text{N}_2$ .

The polymerization of  $\text{S}_2\text{N}_2$  to  $(\text{SN})_x$  can be monitored using ESR techniques. Neither pure  $\text{S}_2\text{N}_2$  nor fully polymerized  $(\text{SN})_x$  has an ESR signal. However, upon bond rupture, a free-radical  $\text{S}_2\text{N}_2$  species might be expected to form from  $\text{S}_2\text{N}_2$  as previously described.<sup>11</sup> It is found that blue-black  $\text{S}_2\text{N}_2$  crystals give a free-radical signal ( $g = 2.005$ ) which initially increases and then decreases with time as polymerization proceeds. Figure 3 shows the time dependence of the ESR signal of an  $\text{S}_2\text{N}_2$  crystalline film which polymerized at room temperature. The data were obtained by allowing the  $\text{S}_2\text{N}_2$  film (originally grown at 77 K) to polymerize at room temperature for the specified period after which the ESR signal was checked at -140 °C by rapidly inserting the sample into the low-temperature ESR cavity. The initial increase in signal intensity is due to an increase in the concentration of the free-radical species and then, as the rate of combination of free radicals into SN polymeric units exceeds the rate at which they are formed, the signal decreases.

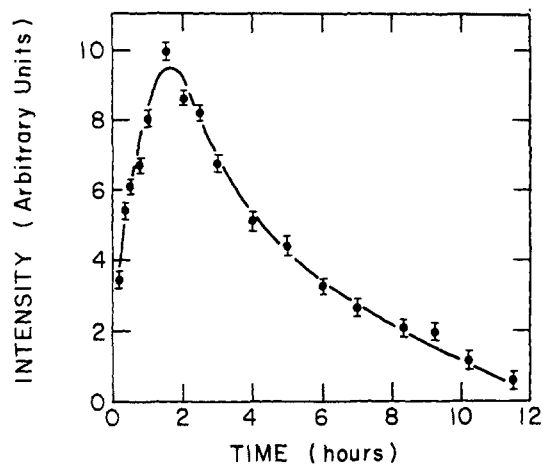


Figure 3. The time dependence of the ESR signal of an  $\text{S}_2\text{N}_2$  crystalline film (measured at -140 °C) polymerized to  $(\text{SN})_x$  at room temperature (see text).

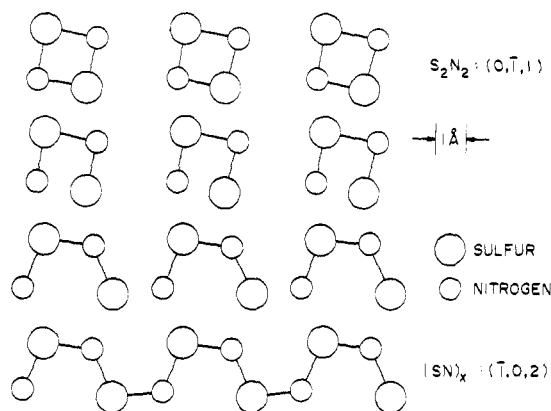
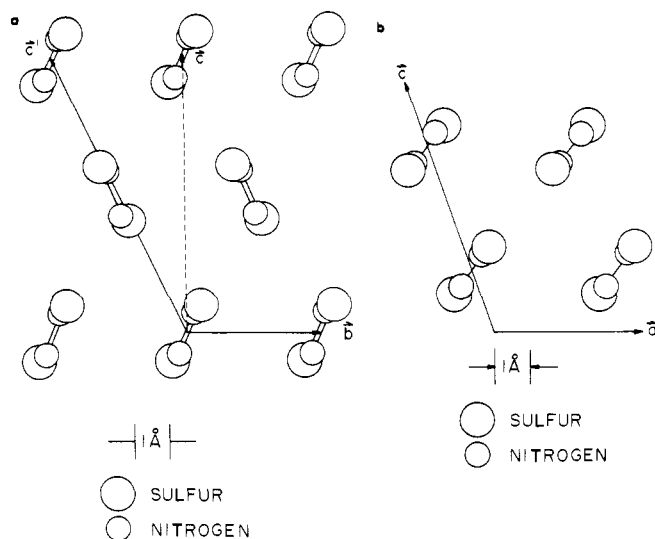


Figure 4. The polymerization of  $\text{S}_2\text{N}_2$  to  $(\text{SN})_x$ . The top view is a projection of the  $\text{S}_2\text{N}_2$  structure onto the  $(0\bar{1}1)$  plane with the  $a$  axis horizontal. The bottom view is a projection of the  $(\text{SN})_x$  structure onto the  $(102)$  plane with the  $b$  axis horizontal. The middle views schematically show the polymerization process.

X-ray measurements for partially polymerized  $\text{S}_2\text{N}_2$  demonstrate the crystallographic  $a$  axis of  $\text{S}_2\text{N}_2$  becomes the  $b$  axis in  $(\text{SN})_x$ ; for example, the  $a$ -axis dimension of 4.460 (4) Å in partially polymerized  $\text{S}_2\text{N}_2$  is not statistically different from the room-temperature  $b$ -axis dimension of 4.439 (5) Å in  $(\text{SN})_x$ . The relative orientation of  $\text{S}_2\text{N}_2$  molecules along the  $a$  axis is the same as the molecular reaction configuration considered previously<sup>11</sup> on the grounds of chemical reasoning alone for the formation of a single  $(\text{SN})_x$  chain.

The proposed polymerization of  $\text{S}_2\text{N}_2$  along the crystallographic  $a$  axis proceeds by an initial ring opening of adjacent  $\text{S}_2\text{N}_2$  molecules to intermediate free-radical  $\text{S}_2\text{N}_2$  species which then covalently bond to form an  $(\text{SN})_x$  polymer chain (Figure 4). The polymerization along the  $a$  axis of  $\text{S}_2\text{N}_2$  and its conversion to the  $b$  axis of  $(\text{SN})_x$  is directly related to the relatively short intermolecular sulfur-nitrogen contact of 2.89 Å observed along the  $a$  axis in the  $\text{S}_2\text{N}_2$  monoclinic phase. Associated with minimum molecular rearrangement during the course of a reaction is the lowest thermodynamic activation free energy. From the point of view of the principle of least atomic motion, the short  $a$ -axis contact in  $\text{S}_2\text{N}_2$  represents a favorable condition for incipient polymerization along the  $a$  axis and subsequent conversion to the  $b$  axis in  $(\text{SN})_x$ .

A series of crystallographic projections of the  $\text{S}_2\text{N}_2$  and  $(\text{SN})_x$  crystal structures are given in Figures 5 and 6 for directly comparing the relative atomic positions and crystallographic symmetry elements for the two crystal structures. In



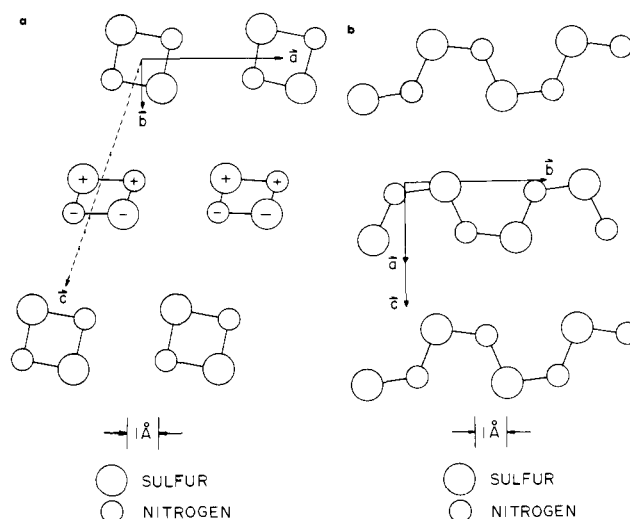
**Figure 5.** (a) The  $S_2N_2$  projected onto a plane perpendicular to the  $a$  axis. See text for explanation of the  $\bar{c}'$  axis. (b)  $(SN)_x$  projected onto the  $(010)$  plane.

Figure 5a, the crystal structure of  $S_2N_2$  is projected perpendicular to the  $a$  axis, which in the monoclinic system is the  $(1, 0, c/a \cos \beta)$  plane. The associated projection for the  $(SN)_x$  structure (Figure 5b) is perpendicular to the  $b$  axis, corresponding to the  $(010)$  projection plane. The relative spatial orientation of the  $S_2N_2$  molecular planes to the  $(SN)_x$  chains as well as the relation between corresponding crystallographic symmetry elements are strikingly similar, suggesting energetically favorable conversion during the reaction process. The axis  $\bar{c}' = (c/a \cos \beta) \bar{a} - \bar{b} + \bar{c}$  shown in the  $S_2N_2$  projection is defined for comparison with the  $(SN)_x$  projection.  $\bar{c}'$  defines a value for  $\beta$  in  $S_2N_2$  of  $114.9^\circ$ . During polymerization the value of  $\beta$  ( $106.43^\circ$ ) of  $S_2N_2$  contracts to  $90^\circ$  allowing the  $\bar{c}'$  axis to become a true symmetry axis; in addition, the row of  $S_2N_2$  molecules located at  $x = 0, y = 1/2$ , and  $z = 1/2$  rotates by  $49^\circ$  about the  $a$  axis. Linear arrays of  $S_2N_2$  molecules along the  $a$  axis can readily polymerize with little or no distortion of the molecular planes, and the formed polymer chains can move along maximum symmetry directions to form the final  $(SN)_x$  structure.

In the  $S_2N_2$  monoclinic phase, the molecules located at  $x = 0, y = 0$ , and  $z = 0$ , and  $x = 0, y = 1$ , and  $z = 1$  lie on the  $(0, \bar{1}, 1)$  plane. This projection together with the  $(\bar{1}02)$  plane projection of  $(SN)_x$  are shown in Figure 6. The rows of  $S_2N_2$  molecules (Figure 6a) are oriented with  $a$  horizontal and the  $(SN)_x$  chains are oriented with  $b$  horizontal. The top and bottom rows of  $S_2N_2$  molecules lie in the plane of the projection while the middle row is rotated  $49^\circ$  out of the plane. Schematically, upon polymerization the middle row of  $S_2N_2$  molecules rotates about the  $a$  axis and all the  $S_2N_2$  rows slip along the  $a$  direction, converting to the  $(SN)_x$  structure. During the course of the actual reaction, the least motion required to form the  $(SN)_x$  lattice consists of simultaneous rotation and translation of rows of  $S_2N_2$  molecules about the crystallographic  $a$  axis (Figure 6).

#### IV. Conclusion

The thermally induced solid state polymerization of  $S_2N_2$  to  $(SN)_x$  arises from the important crystallographic features of the  $S_2N_2$  monoclinic phase described above. As we have noted previously,<sup>11</sup> the S–N bond lengths in  $S_2N_2$  are intermediate between those expected for a single and double bond. It is difficult to estimate the exact extent of  $\pi$  bonding in each S–N linkage since the observed bond length will depend both



**Figure 6.** (a)  $S_2N_2$  projected onto the  $(0\bar{1}1)$  plane. The positive and negative signs designate atoms lying above and below the  $(0\bar{1}1)$  plane, respectively. (b)  $(SN)_x$  projected onto the  $(\bar{1}02)$  plane.

on  $\sigma$  bond contributions, which themselves are dependent in part on the nature of the hybridization both at the sulfur and at the nitrogen atoms, as well as on the extent of  $\pi$  interactions. The bond order may be as high as 1.5 if sulfur d orbitals are involved in the bonding.<sup>11</sup> However, if it is assumed that no d orbitals are involved, as suggested by Patton and Raymond,<sup>14a</sup> then resonance structures such as



must be dominant, suggesting a bond order of 1.25, which would be expected for a 6  $\pi$  aromatic system. This structure would be analogous to cyclobutadiene, but having two filled, instead of two half-filled,  $\pi$  nonbonding degenerate molecular orbitals.<sup>14b</sup> In the  $a$  direction of  $S_2N_2$ , the sulfur–nitrogen intermolecular distance is only 2.89 Å. This overlap suggests a coherent pathway for ring opening as illustrated in Figure 4. However, the question of whether the coherence persists over transverse distances comparable to crystal dimensions is answered by the fact that the resultant crystalline  $(SN)_x$  actually consists of bundles of single crystal fibers only a few hundred angstroms in diameter. In Figure 4, the polymerization could have occurred equivalently with the top rather than the bottom bond opening. The result is that crystalline  $(SN)_x$  samples are often heavily twinned.

The lack of long-range coherence during polymerization is evident in the well-defined defect structure directly observed in the x-ray studies of crystalline  $(SN)_x$ . Fractionally occupied sites are observed in the  $(SN)_x$  x-ray data which correspond to polymer chains structurally out of phase consistent with the combined symmetries of  $(SN)_x$  and the precursor  $S_2N_2$ .<sup>15</sup> As a result, the solid-state polymerization of the monoclinic phase of  $S_2N_2$  to  $(SN)_x$  as described above makes practically unavoidable the defect structure in the form of characteristic fiber bundles and consequent strong surface striations in presently available  $(SN)_x$  material.

Both partially polymerized  $S_2N_2$  and  $(SN)_x$  have well-defined defect structures in the form of periodic interstitial atomic sites. These defect structures have been used by Baughman et al.<sup>15</sup> in a least motion calculation which verifies the polymerization model presented here.

The minimum sulfur–sulfur and sulfur–nitrogen distances between adjacent  $(SN)_x$  chains parallel to the  $(102)$  plane are 3.476 (4) and 3.256 (7) Å, respectively. The minimum sulfur–sulfur and sulfur–nitrogen distances between adjacent

(SN)<sub>x</sub> chains not in the same plane are 3.721 (4) and 3.396 (7) Å, respectively. These may be compared with the approximate van der Waals radii of 3.70 and 3.35 Å for sulfur–sulfur and sulfur–nitrogen contacts, respectively. Band structure calculations<sup>16</sup> based either on the x-ray structure presented here or on the trial structure inferred from electron-diffraction studies suggest that the electronic overlap between chains is important and arises from both sulfur–sulfur and sulfur–nitrogen interactions. The structural rearrangements that occur during polymerization give direct evidence for strong interchain interactions in (SN)<sub>x</sub>. As a result, there is a rotation about *a* to convert the herring-bone structure of S<sub>2</sub>N<sub>2</sub> to the (102) planar structure of (SN)<sub>x</sub>.

The atoms in the (SN)<sub>x</sub> polymer chain (*z* axis in the direction of the chain) lie in the *yz* plane. The bond lengths in (SN)<sub>x</sub> are very nearly equivalent, 1.593 (5) and 1.628 (7) Å,<sup>11</sup> and are intermediate between those expected for a single and a double sulfur–nitrogen bond.<sup>11</sup> The bond angle at the nitrogen atoms (119.9°) suggests sp<sup>2</sup> hybridization involving the two S–N σ bonds and the lone pair nitrogen electrons in the *yz* plane. In this bonding model, the fifth nitrogen valence electron is depicted as being present in a p<sub>x</sub> atomic orbital perpendicular to the (SN)<sub>x</sub> chain. The angle at the sulfur atoms (106.2°) indicates approximate tetrahedral hybridization which will involve the two S–N σ bonds in the *yz* plane and the two sulfur lone pair orbitals directed above and below this plane. While not strictly valid in the solid state because of S–N interactions along the chain, the traditional hybridization concept provides a useful starting point for formulating an approximate, qualitative model of the bonding in (SN)<sub>x</sub>.<sup>11</sup> Sulfur d orbital participation<sup>11</sup> is not included for simplicity.

Considering only s and p orbitals, a hyperconjugative π bonding interaction<sup>17</sup> between the half-filled nitrogen p<sub>x</sub> orbital and the filled sulfur sp<sup>3</sup> lone pair orbitals of appropriate symmetry will result in some multiple bond character in each S–N bond. The eleventh valence electron formally associated with each SN unit can then be accommodated in the π\* orbital associated with the hyperconjugative π bond. Overlap of the π\* orbitals of each SN unit in the polymeric (SN)<sub>x</sub> can result in the metallic conduction band.

It seems possible that the proposed interaction between sulfur atoms in adjacent (SN)<sub>x</sub> chains parallel to the (102) plane<sup>15,16,18</sup> could occur by an interaction of the sulfur sp<sup>3</sup> lone pair orbitals which are pointed toward each other. Their partial depopulation by interaction with the half-filled p<sub>x</sub> orbital on each nitrogen could result in a bonding interaction between the sulfur atoms in these adjacent chains. The sulfur–nitrogen interaction in this plane could involve, at least in part, the overlap of the nitrogen lone pair with an empty σ\* orbital associated with the nearest sulfur in an adjacent chain. The interaction between chains in different planes could arise from interactions between the π systems. These interactions between SN chains would appear to contribute to the force responsible for rotating the chains (Figures 5 and 6) so that they are coplanar in the (SN)<sub>x</sub> structure. Additional contributions to interchain interaction can arise from ionic coupling associated with the asymmetric charge distribution of each SN unit.<sup>15,16</sup>

The interatomic distances in (SN)<sub>x</sub> and the interactions calculated from them bear directly on the question of whether in fact (SN)<sub>x</sub> is to be viewed as a one-dimensional metal. The

lack of evidence of a Peierls–Fröhlich instability suggests that interchain coupling may be important. The anisotropy of the optical reflectance,<sup>6</sup> the thermopower,<sup>19</sup> and the electrical conductivity<sup>8</sup> indicate that (SN)<sub>x</sub> is more likely an anisotropic metal with sufficient electronic interchain coupling to quench the Peierls distortion. These observations are consistent with electron energy loss measurements<sup>20</sup> of the anisotropic plasmon spectrum.

**Acknowledgment.** We gratefully acknowledge many stimulating and helpful discussions with Dr. R. Baughman on the x-ray structure and the solid-state polymerization process. The cooperation of the Molecular Structure Corporation and their careful experimental work made this study possible.

**Supplementary Material Available:** tables of structure factor data, positional and thermal parameters, least-squares planes, and structure factor amplitudes (55 pages). Ordering information is given on any current masthead page.

## References and Notes

- (1) This research was supported by the National Science Foundation through the Laboratory for Research on the Structure of Matter, DMR-22923, GP-41766X, and by the Advanced Research Projects Agency through DAHC 15-72C-0174.
- (2) (a) Department of Physics; (b) Department of Chemistry; (c) Laboratory for Research on the Structure of Matter.
- (3) (a) V. V. Walatka, Jr., M. M. Labes, and J. H. Perlstein, *Phys. Rev. Lett.*, **31**, 1139 (1973); (b) R. L. Greene, P. M. Grant, and G. B. Street, *ibid.*, **34**, 89 (1975).
- (4) See, for example, A. F. Garito and A. J. Heeger, "Collective Properties of Physical Systems", S. Lundquist, Ed., Nobel Press, 1974; A. F. Garito and A. J. Heeger, *Acc. Chem. Res.*, **7**, 232 (1974), and references therein.
- (5) See, for example, W. Glaser, "Festkörperprobleme XIV", H. J. Queisser, Ed., Pergamon/Vieweg 1974, p 205, and references therein.
- (6) (a) A. A. Bright, M. J. Cohen, A. F. Garito, A. J. Heeger, C. M. Mikulski, P. J. Russo, and A. G. MacDiarmid, *Phys. Rev. Lett.*, **34**, 206 (1975); (b) A. A. Bright, M. J. Cohen, A. F. Garito, A. J. Heeger, C. M. Mikulski, and A. G. MacDiarmid, *Appl. Phys. Lett.*, **26**, 612 (1975).
- (7) R. L. Greene, G. B. Street, and L. J. Suter, *Phys. Rev. Lett.*, **34**, 577 (1975).
- (8) M. J. Cohen, C. K. Chiang, A. F. Garito, A. J. Heeger, P. J. Russo, C. M. Mikulski, and A. G. MacDiarmid, *Bull. Am. Phys. Soc.*, **20**, 360 (1975); C. K. Chiang, M. J. Cohen, A. F. Garito, A. J. Heeger, C. M. Mikulski, and A. G. MacDiarmid, *Solid State Commun.*, in press; W. D. Gill, P. M. Grant, R. L. Greene, and G. B. Street, *Phys. Rev. Lett.*, **35**, 1732 (1975).
- (9) C. H. Hsu and M. M. Labes, *J. Chem. Phys.*, **61**, 4640 (1974).
- (10) A. G. MacDiarmid, C. M. Mikulski, P. J. Russo, M. S. Saran, A. F. Garito, and A. J. Heeger, *Chem. Commun.*, 476 (1975).
- (11) C. M. Mikulski, P. J. Russo, M. S. Saran, A. G. MacDiarmid, A. F. Garito, and A. J. Heeger, *J. Am. Chem. Soc.*, **97**, 6358 (1975).
- (12) Molecular Structure Corporation, College Station, Tex. 77840.
- (13) M. Boudeulle, Ph.D. Thesis, University Claude-Bernard de Lyon, 1972; M. Boudeulle, *Cryst. Struct. Commun.*, **4**, 9 (1975).
- (14) (a) R. L. Patton and K. N. Raymond, *Inorg. Chem.*, **8**, 2426 (1969), and references therein; (b) K. N. Raymond, private communication, 1976.
- (15) R. Baughman, R. R. Chance, and M. J. Cohen, *J. Chem. Phys.*, **64**, 1869 (1976); R. H. Baughman and R. R. Chance, preprint.
- (16) H. Kamimuro, A. J. Grant, F. Levy, A. D. Yoffe, and G. D. Pitt, *Solid State Commun.*, **17**, 49 (1975); D. E. Parry and J. M. Thomas, *J. Phys. C.*, **8**, L45 (1975); W. I. Friesen, A. J. Berlinsky, B. Bergersen, L. Weiler, and T. M. Rice, preprint; V. T. Rajan and L. M. Falicov, *Phys. Rev. B*, **12**, 1240 (1975); W. E. Rudge and P. M. Grant, *Phys. Rev. Lett.*, **35**, 1799 (1975); A. A. Bright and P. Soven, *Solid State Commun.*, **1B**, 317 (1976); R. P. Messmer and D. R. Salahub, in press; D. R. Salahub and R. P. Messmer, in press.
- (17) M. J. S. Dewar, "Hyperconjugation", Ronald Press, New York, N.Y., 1962; A. Streitwieser, Jr., "Molecular Orbital Theory for Organic Chemists", Wiley, New York, N.Y., 1967; J. N. Murrell, S. F. A. Kettle, and J. M. Tedder, "Valence Theory", Wiley, New York, N.Y., 1965.
- (18) For a diagrammatic representation of the S–S interaction in the (102) plane, see A. G. MacDiarmid, C. M. Mikulski, M. S. Saran, P. J. Russo, M. J. Cohen, A. A. Bright, A. F. Garito, and A. J. Heeger in "Inorganic Compounds with Unusual Properties", *Adv. Chem. Ser.*, in press.
- (19) M. J. Cohen, Ph.D. Thesis, University of Pennsylvania, 1975.
- (20) C. H. Chen, J. Silcox, A. F. Garito, A. J. Heeger, and A. G. MacDiarmid, *Phys. Rev. Lett.*, **36**, 525 (1976).